

# Retrieval of BRDF for pure landcover types from MODIS and MISR using an angular unmixing approach

Alexander P. Trishchenko<sup>\*a</sup>, Konstantin Khlopenkov<sup>a</sup>, Yi Luo<sup>b</sup>

<sup>a</sup>Canada Centre for Remote Sensing, 588 Booth St, Ottawa, ON Canada K1A0Y7;

<sup>b</sup>Noetix Research Inc., Ottawa, ON Canada

## ABSTRACT

Information about the surface bi-directional reflectance distribution function (BRDF) and albedo is required as a boundary condition for radiative transfer modeling, aerosol retrievals, cloud retrievals, and atmospheric modeling. The typical spatial resolution provided by MODIS and MISR standard surface products (~1km) is insufficient to measure the BRDF of the pure surface types, because most pixels at this scale correspond to mixed classes. We present an approach for the retrieval of the basic surface BRDFs from the observations of MODIS/Terra and MISR using an angular unmixing method. Our analysis is focused on the Atmospheric Radiation Measurement (ARM) Program area in the Southern Great Planes (SGP) region, which is a predominantly agricultural area with a few major crop types. Pure surface classes were identified using high-resolution (30m) Landsat imagery and results of a ground survey.

Assuming that the reflectance for each coarse pixel is a linear superposition of reflectances of basic surface types, it is possible to estimate the original BRDF parameters for each landcover type. In our case, three dominant classes were selected: wheat, grass, and baresoil. In the case of wheat and grass, the dispersion of the results is smaller than in the case of soil. This can be explained by the relatively low fractional coverage of the soil class within large pixels and by the significant variability of soil reflectance depending on wetness, soil type (sand, clay, etc.), and other factors. The correlation between the BRDF shape factors and the normalized difference vegetation index (NDVI) has also been analyzed. There is a high degree of correlation between the NDVI and BRDF isotropic factor ( $r_0$  in the case of MISR), while the correlation with other BRDF parameters was found to be smaller. In general, the NDVI can be used as a crude proxy for the BRDF shape.

**Keywords:** remote sensing, BRDF, MODIS, MISR, angular unmixing.

## 1. INTRODUCTION

The bi-directional reflectance distribution function (BRDF) determines the degree of anisotropy of the surface's reflective properties<sup>1</sup>. This is a basic parameter employed in the vegetation structure retrievals and characterization of surface albedo. An important feature of the BRDF shape is the amplitude and width of the hot spot and dark spot areas in the principle plane direction. The general BRDF shape in the direction of the perpendicular plane is also important. Retrieving the BRDF shape from a satellite observation is a difficult task<sup>2</sup>. In general, satellite sensors do not provide simultaneous measurements of reflectance in all viewing directions. For example, in BRDF retrievals from MODIS observations<sup>2-3</sup>, angular coverage is achieved by assembling clear-sky pixels from different orbits within a certain interval of time: 8, 10, or 16 days. Multiangular observations from MISR contain simultaneous measurements at nine viewing directions, thus providing much better capabilities for surface BRDF retrievals and an atmospheric correction for the presence of the atmospheric aerosols. However, since MISR has a narrow swath and operates on sun-synchronous orbit, it cannot provide complete angular coverage for the entire angular domain<sup>2</sup>. Thus, having the BRDF models for generic landcover types could be important. These generic models could be adjusted for each particular case, based on a limited sample of angular measurements.

To construct the generic BRDF for a specific landcover type, one needs to ensure an adequate sampling of observations in the viewing zenith angle vs. relative azimuth angle (VZA-RAA) plane for various ranges of the solar zenith angle

---

\* trichtch@ccrs.nrcan.gc.ca; phone 1 613 995-5787; www.ccrs.nrcan.gc.ca.

(SZA). The best strategy to achieve this task is to collect all of the reflectance data for all of the pixels with the same landcover type, and then use these data to derive the generic BRDF shape<sup>2</sup>. In reality, however, the definition of landcover type may not be a perfect identification of the type of surface element, from the BRDF point of view. For example, “cropland” is a frequently used landcover type to denote a large variety of vegetation types, such as wheat, corn, soybeans, and many others. Depending on the season, the area identified as cropland may correspond also to baresoil or the mixed conditions – baresoil and vegetation. Another problem is related to the mixing of various landcover types within one pixel. If the pixel size is larger than the typical size of agricultural fields, then the pixel contains a mixture of various fields. Also, there is a problem associated with similar landcover types in different conditions and/or stages of growth. Although identical in the landcover type, their BRDF properties may look very different.

Below, we present some of the results of our analysis aimed at studying the problem of the mixing of various landcover types and how this affects the BRDF at a coarse spatial resolution. In particular, we analyzed MODIS and MISR observations and deduced the BRDFs for pure landcover types using the angular unmixing method. We also studied the relationship between the BRDF shape of mixed landcover classes and the level of the NDVI.

## 2. ANGULAR UNMIXING

### 2.1. General procedure

The area of interest encompasses the region of approximately 20×20 km<sup>2</sup> around the Atmospheric Radiation Measurement (ARM) Program Southern Great Plains (SGP) Central Facility (CF) located in Northern Oklahoma, USA. LANDSAT data were used to produce landcover maps with 30m spatial resolution. At this spatial resolution, the majority of pixels correspond to the pure landcover types (such as wheat, grass, baresoil, etc.). The digital landcover map was created first by conducting an unsupervised classification for a large number of classes. The classes were then aggregated to a smaller number of landcover types using the results of the ground survey. An example of the landcover map derived from LANDSAT is shown in Fig. 1. The number of classes on the map was reduced to three dominant classes representing >90% of the area. All of the other types were grouped into the 4th class, “others”. The map corresponds to the mid-May conditions in 2003. It’s accuracy is estimated to be better than 95%.

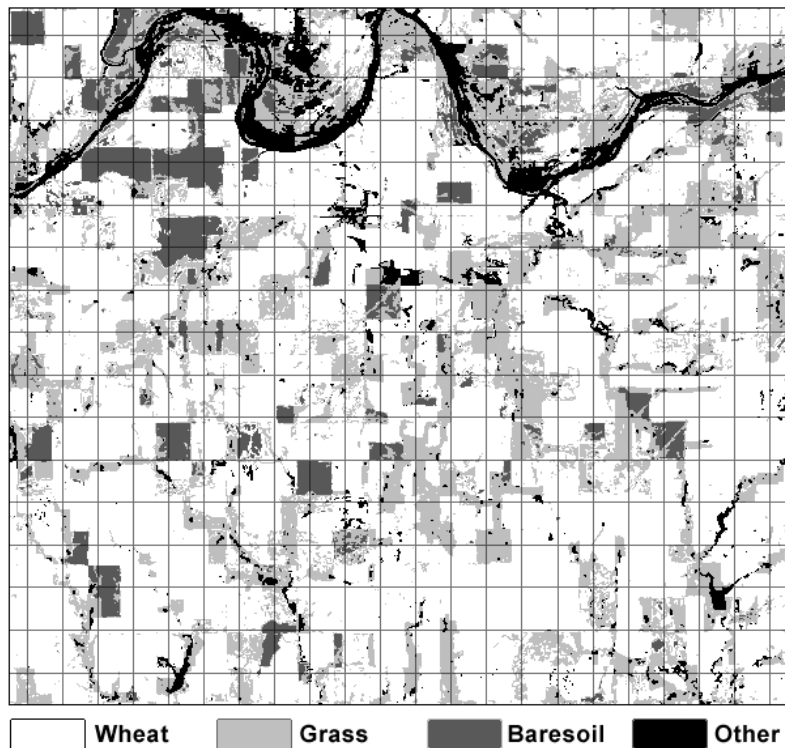


**Fig. 1.** Example of the landcover map for SGP area derived from a LANDSAT TM image and ground survey. The rectangular grid shows the location of MISR pixels.

The MODIS and MISR images are used to produce surface BRDF/Albedo on regular basis<sup>2,4</sup>. The typical spatial resolution for MODIS and MISR product is approximately 1 km. Unlike LANDSAT, almost all of the pixels in the MODIS and MISR product for the area shown in Fig. 1 represent mixed landcover types. The rectangular grid on Fig. 1 denotes the location of pixels from the MISR Level-2 surface product (version 15). The MODIS data product generated for 10-day intervals at 500m spatial resolution<sup>2</sup> was also employed in this study.

The hemispheric backscattering albedo of the atmosphere under clear sky conditions is very small, and one can neglect the effects of multiple backscattering of the surface reflected radiation (adjacency effect). With this assumption, the total radiation reflected from a coarse resolution pixel can be considered as linear integral over the subpixels. Therefore, the reflectance  $R$  of a pixel  $i$  containing a mixture of landcover types can be represented as a linear sum of reflectances  $r_c$  for each cover class  $c$ :

$$R_i(\theta_0, \theta, \phi, \lambda) = \sum_c w_{c,i} r_c(\theta_0, \theta, \phi, \lambda), \quad (1)$$

where  $\theta_0, \theta$  are the sun and view zenith angles,  $\phi$  is the relative azimuth angle,  $\lambda$  is the wavelength or spectral band, and  $w_{c,i}$  is the weight of each class, i.e., the fractional coverage of the landcover class  $c$  for pixel  $i$ , with  $\sum_c w_c = 1$ .

LANDSAT-derived map was used to obtain weights  $w_c$ .

Initially, for our analysis, we selected five distinct landcover classes present in the ARM SGP area: wheat, grass, baresoil, trees/shrubs, and water. Taking a group of MODIS or MISR pixels and writing Eq. (1) for each pixel, a set of linear equations was built with the five unknowns,  $r_c$ . Unknowns  $r_c$  represent the average reflectances of each landcover class. To reduce the impact of low-scale variability, we analyzed data by grouping several coarse resolution pixels together. The solution was derived using a least-squares fit since the number of unknowns was less than the number of equations. To reduce the noise and still produce enough data for building reliable statistics, we used groups ranging from 12 to 16 pixels. Since the trees/shrubs and water landcover classes have typically a very low abundance in the SGP area, the retrievals for these classes contain a high level of noise. As such, they were excluded from the subsequent analysis.

## 2.2. MODIS data

We used the MODIS landcover-based fitted (LBF) BRDF data product produced by Luo et al.<sup>2</sup> It contains three parameters for each of the seven spectral bands. The parameters are mapped on a spatial grid with 500m spatial resolution. These three parameters are the coefficients of the RossThick – LiSparse model<sup>5</sup>, which expands the BRDF into a linear sum of three kernels: isotropic (*ISO*), volume-scattering (*VOL*), and geometric-optical (*GEO*):

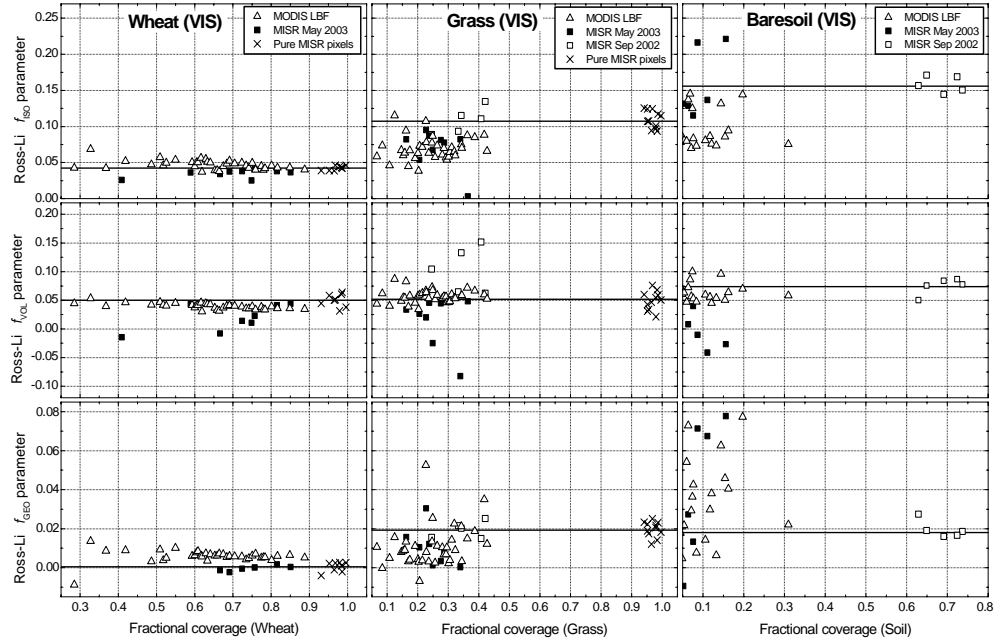
$$R_i(\theta_0, \theta, \phi, \lambda) = f_{ISO}(\lambda) + f_{VOL}(\lambda)K_{VOL}(\theta_0, \theta, \phi) + f_{GEO}(\lambda)K_{ISO}(\theta_0, \theta, \phi) \quad (2)$$

where  $K_{VOL}(\theta_0, \theta, \phi)$  and  $K_{ISO}(\theta_0, \theta, \phi)$  are the kernel functions of the model, and  $f_k$  are the model parameters.

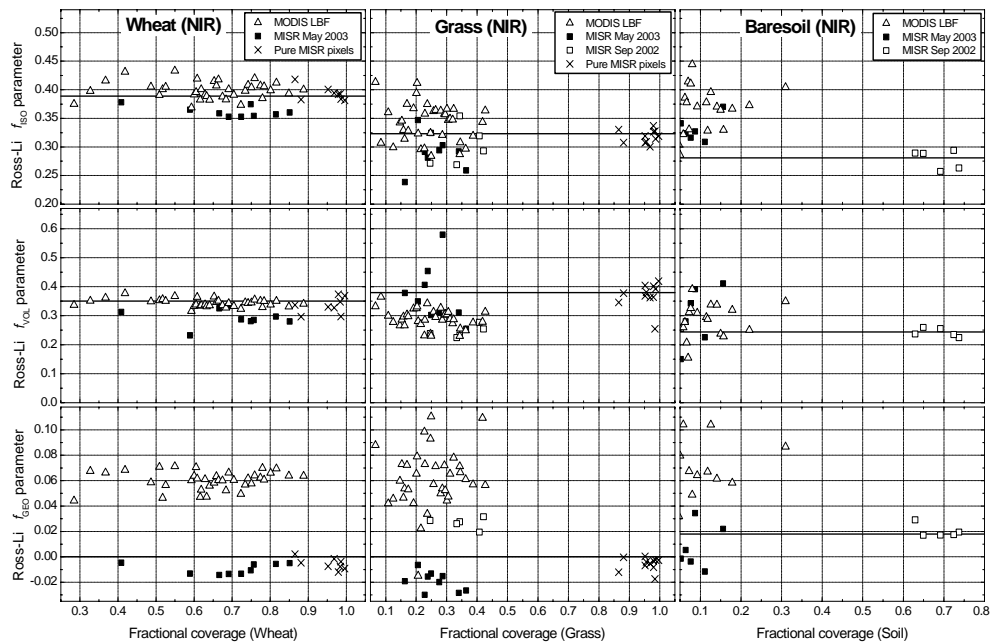
Due to the linearity of the BRDF model, the unmixing method as described above can be applied directly to the parameters  $f_{ISO}$ ,  $f_{VOL}$ , and  $f_{GEO}$ . For each group of pixels, we can obtain the three parameters of the Ross-Li model that correspond to the average reflectance of the pure landcover classes.

Fig. 2 presents the result of the linear unmixing for the MODIS red channel (620–670 nm). Each panel on Fig. 2 shows the parameter derived for each landcover class for all pixel groups. The horizontal axes show the fractional coverage of a particular class within the pixel group. For example,  $x$  values close to 1 correspond to pixels with a pure landcover type. It is seen that the scattering of the parameters becomes smaller when the fractional coverage is higher. Larger scattering for small fractional coverage probably occurs due to small-scale surface inhomogeneities and uncertainties in image registration for the coarse resolution pixel, when an insignificant mismatch in the pixel location has a large impact on the small fraction of the area. The plot also includes the values obtained by fitting the MISR data with the Ross-Li BRDF model. The details of this procedure are explained in the next section. The smallest scattering is achieved for the wheat landcover type for all three model parameters. A larger scattering is observed for the grass landcover type. This can be presumably explained by the higher variability in the reflective properties for grass fields.

The largest scattering of the retrieval results is observed for the baresoil landcover type. This may be attributed to the high variability of the reflectance for this landcover class, which in many cases can be a mixture of dry grass, corn stalks, and open soil. Another contributing factor is the low abundance of this class in the spring season. This is confirmed by the results of the analysis for the Fall 2002, when baresoil, which replaces wheat fields, becomes a dominant class.



**Fig. 2.** Results of linear unmixing for the red spectral band. Open triangles correspond to the model parameters for MODIS<sup>2</sup>. Squares correspond to MISR data fit. Pure pixels are shown as crosses. Solid lines show the weighed average values for pure landcover types.



**Fig. 3.** Similar to Fig.2, but for the NIR channel.

A similar set of graphs is shown in Fig. 3 for the near infrared (NIR) channel (841–876 nm). Some differences were found between the values of  $f_{\text{GEO}}$  derived from MODIS and those obtained by fitting the BRDF model to the multiangular reflectance data of MISR for pixels with pure classes. This discrepancy is observed for all three landcover classes and is associated with the constrained fitting of MODIS data, when the parameters are assumed to be non-negative. Unconstrained fitting of MISR data by the Ross-Li model frequently leads to the negative, non-physical solution for  $f_{\text{GEO}}$ , which is usually the smallest among all three parameters.

### 2.3. Unmixing of MISR data

The MISR dataset contains several layers of data. We used the Bidirectional Reflectance Factor (BRF)<sup>5</sup>, defined as the surface-leaving radiance divided by the radiance from a lambertian reflector illuminated from a single direction. The BRF layer contains data images with 1.1km per pixel spatial resolution where each pixel has values of reflectance measured from nine different directions (with negligible time lag) in four spectral channels<sup>4</sup>.

The application of the unmixing method is also possible for the multiangular MISR data, but the routine is slightly more complicated. Considering one spectral channel and one direction (described by the view angle  $\theta$  and the relative azimuth angle  $\phi$ ), we can again write equation (1) for the reflectance of each MISR pixel. Combining several pixels in one group, one can build the overdetermined set of linear equations. This set can again be solved using the least-squares method for the five unknown values of the characteristic reflectances of each landcover class. Repeating the procedure for each direction, we can collect nine values of reflectance for each group of pixels.

It is also possible to use more than one MISR orbit over the region of interest in order to collect more values of directional reflectance measured at different directions. The data must be taken within short period of time and correspond to cloud-free conditions. In the case of the May 2003 data series, only one satellite pass was available, whereas in case of September 2002, it was possible to use two passes within a nine-day interval.

Having collected several values of directional reflectance, it is possible to fit a BRDF model to these data. We limited our analysis to two BRDF models: the RossThick–LiSparse model<sup>5</sup> (see Eq. 2), and the modified Rahman model<sup>4,6</sup>, employed in the MISR data processing, as defined by Eq.3 below:

$$R(\theta_0, \theta, \phi) = r_0 (\cos \theta \cos \theta_0 (\cos \theta + \cos \theta_0))^{k-1} h \exp(-b \cos \xi) \quad (3)$$

$$h(\theta_0, \theta, \phi) = 1 + \frac{1 - r_0}{1 + G(\theta_0, \theta, \phi)}$$

$$G(\theta_0, \theta, \phi) = \sqrt{\tan^2 \theta + \tan^2 \theta_0 - 2 \tan^2 \theta \tan^2 \theta_0 \cos \phi}$$

$$\cos \xi = \cos \theta \cos \theta_0 + \sin \theta \sin \theta_0 \cos \phi$$

where  $r_0$ ,  $k$ , and  $b$  are the three fitting parameters of the model, responsible for the amplitude of the BRDF, its overall shape and the hot spot area, respectively.

The obtained sets of multiangular data were fitted using the Levenberg-Marquardt method<sup>7</sup> of non-linear least-squares fitting of multi-dimensional functions. Fig. 4 presents the comparison of the fitted models with the observed multiangular reflectances for selected MISR pixels that represent pure landcover classes. It should be noted that the MISR measurements do not lie in the principal plane, but at about 45° relative to the principal plane. For this reason, the hot spot area ( $\theta_0 = 23.5^\circ$  for this case) is not well defined.

For each pixel group, we obtained the three model parameters  $r_0$ ,  $k$ , and  $b$  for each landcover class. The fitting procedure was applied to each pixel group with different fractional coverage of the landcover classes. The results of the fitting for the red MISR channel (672 nm) are shown in Fig. 5. Again, it is seen that there is less scattering of the parameters for the higher fractional coverage. A similar set of graphs for the near infrared (NIR) channel (866 nm) is shown in Fig. 6.

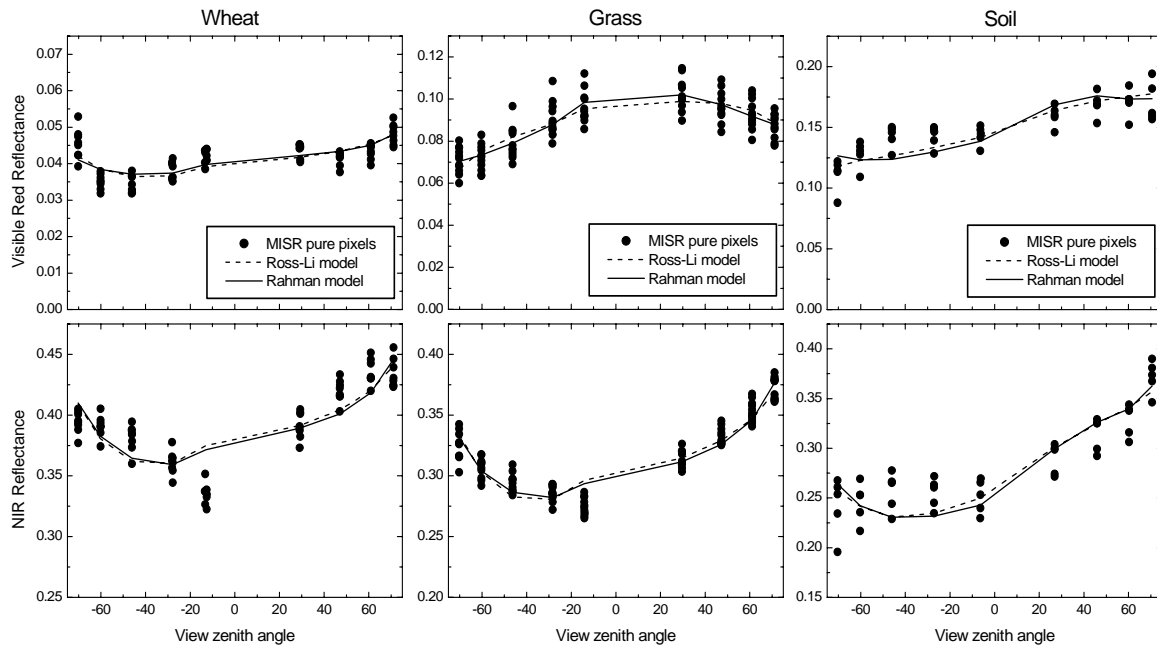


**Fig. 4.** Fitting the MISR reflectances with the Ross-Li and modified Rahman models for the pixels with pure landcover types: grass, wheat, soil.

The relationship between the BRDF model parameters and the NDVI index for pure MISR pixels is presented in Fig. 7. Analysis of BRDF parameters against the NDVI suggests that the NDVI index has the most significant impact on the overall amplitude of the reflectance. The geometric  $f_{GEO}$  and volumetric  $f_{VOL}$  parameters of the Ross-Li and  $k$  and  $b$  parameters of the modified Rahman model show a relatively weak correlation with NDVI for the considered landcover types and scenes.

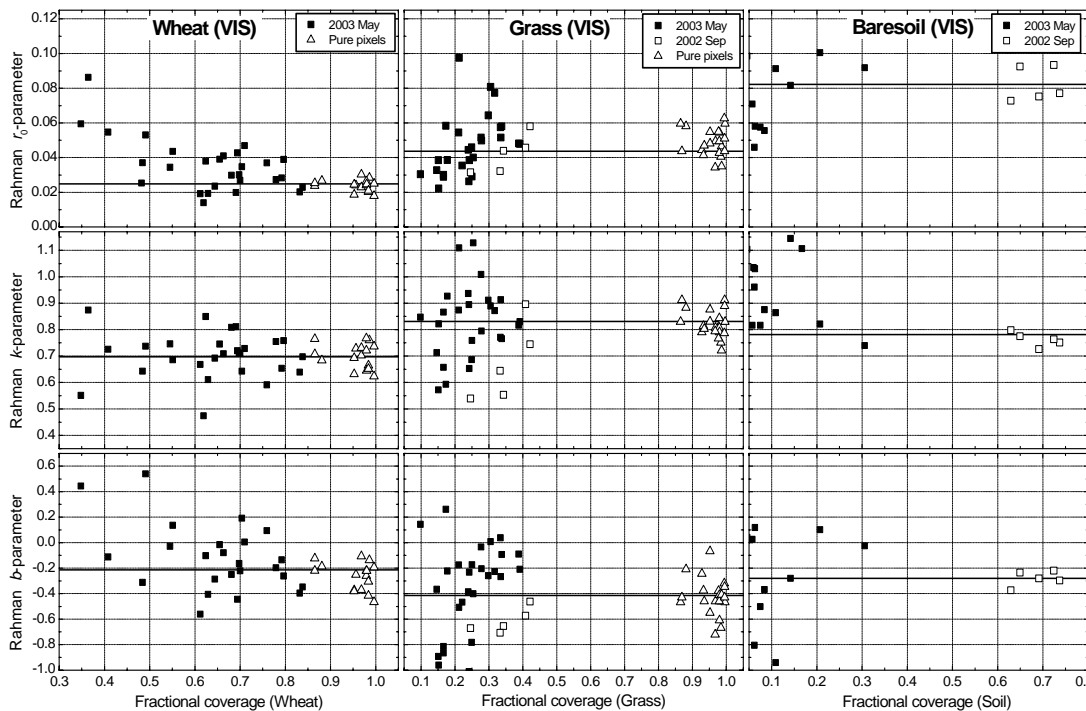


**Fig. 5.** Rahman model parameters for the red spectral band. Data for MISR pixels with low fractional coverage are shown as squares. Pure pixels are shown as triangles. Solid lines show the weighed average values for pure pixels.

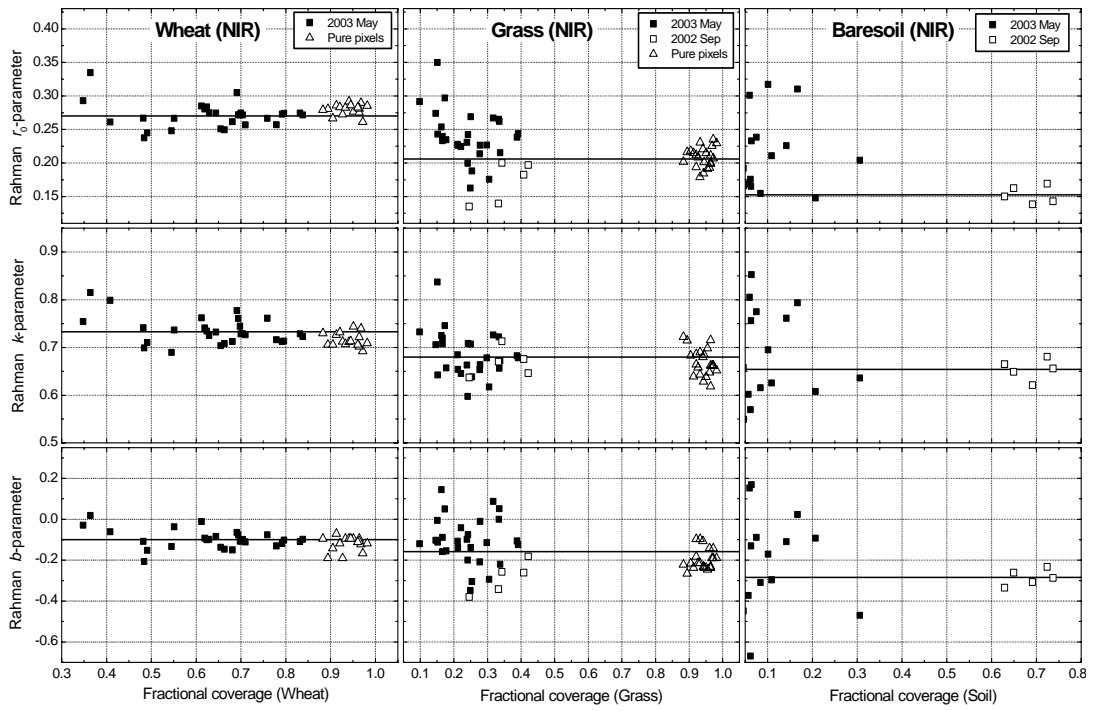


Fig. 6. Same as in Fig.5, but for the NIR channel.

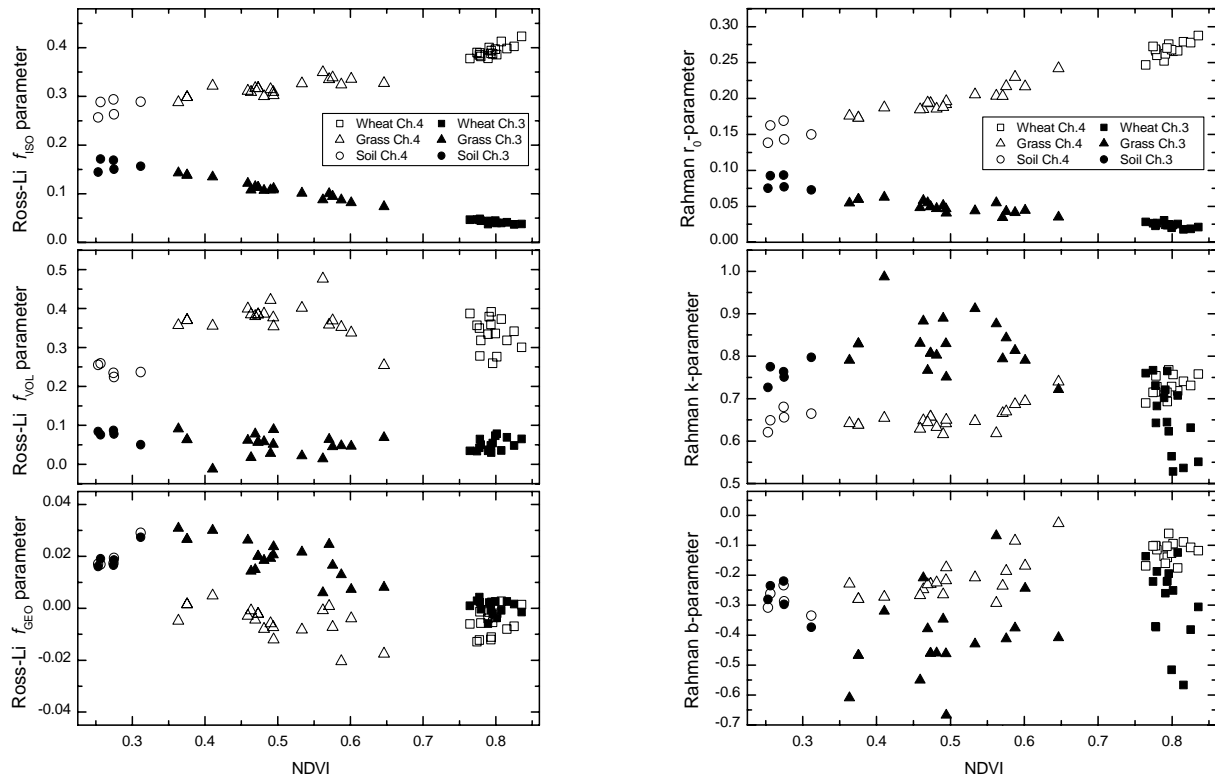


Fig. 7. Comparison of fitted model parameters with the NDVI for pure MISR pixels for ch.3 (red) and ch.4 (NIR). Unconstrained fitting leads to negative  $f_{GEO}$ .

### 3. CONCLUSION

A high-spatial resolution landcover map of the agricultural area in the ARM SGP area was produced from LANDSAT data and was used to study the BRDF properties of pure and mixed landcover types employing MODIS and MISR data. Two BRDF models were used: the Ross-Li model and the modified Rahman model. Neglecting the adjacency effect at 500m–1km scale, we assumed the linear mixing model, which can be inverted using least-squares fitting.

In general, our approach produces results consistent with independent analysis based on ground observations. Linear unmixing can be applied to deduce the BRDF properties of pure classes. The uncertainty of this approach becomes smaller when the fractional area or the particular class increases.

In case of the NIR channel, the  $k$ -parameter is higher for wheat than for grass, while in the visible red channels, the picture is reversed. In general, the variability of the retrieved parameters for wheat is smaller, and for bare soil, it is the highest. The latter is especially true when this class represents low fractional coverage.

Analysis of BRDF parameters against the NDVI suggests that the NDVI can be used as the parameter for the separation/aggregation of pixels in the BRDF fitting procedure independent on the specific type of vegetation (grass, wheat, soil, or mixture of the above), since it affects mostly the amplitude but not the shape of the BRDF for cropland types.

### ACKNOWLEDGEMENT

This research was supported by the US Department of Energy Atmospheric Radiation Measurement (ARM) Program under grant No. DE-FG02-02ER63351.

### REFERENCES

1. F. E. Nicodemus, J. C. Richmond, J. J. Hsia, I. Ginsberg, and T. Limperis. *Geometric considerations and nomenclature for reflectance*. U. S. Dept. of Commerce, NBS Monograph. 1977.
2. Y. Luo, A. P. Trishchenko, R. Latifovic, and Z. Li. Surface bidirectional reflectance and albedo properties derived by a landcover based approach from the MODIS observations, *J. Geophys. Res. (submitted)*, 2004.
3. C. B. Schaaf, F. Gao, A. H. Strahler, W. Lucht, X. Li, T. Tsang, N. C. Strugnell, X. Zhang, Y. Jin, J.-P. Muller, P. Lewis, M. Barnsley, P. Hobson, M. Disney, G. Roberts, M. Dunderdale, C. Doll, R. d'Entremont, B. Hu, S. Liang, and J. L. Privette. First operational BRDF, albedo and nadir reflectance products from MODIS, *Remote Sens. Environ.*, 83, 135–148, 2002.
4. D. J. Diner, J. V. Martonchik, C. Borel, S. A. W. Gerstl, H. R. Gordon, Y. Knyazikhin, R. Myneni, B. Pinty, and M. Verstraete, MISR level 2 surface retrieval, *Report of JPL D-11401*, 1999. ([http://eosps0.gsfc.nasa.gov/eos\\_homepage/for\\_scientists/atbd/docs/MISR/atbd-misr-10.pdf](http://eosps0.gsfc.nasa.gov/eos_homepage/for_scientists/atbd/docs/MISR/atbd-misr-10.pdf)).
5. W. Wanner, X. Li, and A. H. Strahler. On the derivation of kernels for kernel-driven models of bi-directional reflectance *J. Geophys. Res.*, 100, 21077–21090, 1995.
6. H. Rahman, B. Pinty, and M. Verstraete. Coupled surface atmosphere reflectance (CSAR) model, 2, Semiempirical surface model usable with NOAA Advanced Very High Resolution Radiometer data, *J. Geophys. Res.*, 98, 20,791–20,801. 1993.
7. W.H. Press, S.A. Teukolsky, W.T. Vetterling, and B.P. Flannery, *Numerical Recipes in FORTRAN: The Art of Scientific Computing*, 2<sup>nd</sup> Ed., Cambridge University Press, Cambridge, 675–683, 1992.